PCCP

Accepted Manuscript

This is an *Accepted Manuscript*, which has been through the Royal Society of Chemistry peer review process and has been accepted for publication.

Accepted Manuscripts are published online shortly after acceptance, before technical editing, formatting and proof reading. Using this free service, authors can make their results available to the community, in citable form, before we publish the edited article. We will replace this *Accepted Manuscript* with the edited and formatted *Advance Article* as soon as it is available.

You can find more information about *Accepted Manuscripts* in the Information for Authors.

Please note that technical editing may introduce minor changes to the text and/or graphics, which may alter content. The journal's standard Terms & Conditions and the Ethical guidelines still apply. In no event shall the Royal Society of Chemistry be held responsible for any errors or omissions in this *Accepted Manuscript* or any consequences arising from the use of any information it contains.

ROYAL SOCIETY OF CHEMISTRY

www.rsc.org/pccp

Magnetic Properties of C-N planar structures: d^0 ferromagnetism and half-metallicity

W. H. Brito,[1,*] Joice da Silva-Araújo,[2] and H. Chacham[1]

[1] *Departamento de Física, Universidade Federal de Minas Gerais, C. P. 702, 30123-970, Belo Horizonte, MG, Brazil.*

[2] *Departamento de Física e Química, Pontifícia Universidade Católica de Minas Gerais, 30535-901, Belo Horizonte, MG, Brazil.*

We investigate, from first principles calculations, the magnetic properties of planar carbon nitride structures with the lowest formation energies within twenty eight distinct stoichiometries and porosities. Surprisingly, we find that 3/4 of the low-energy carbon nitride structures present energetically favorable magnetic phases, and that more than 3/10 are ferromagnetic. This suggests that d^0 magnetism is an usual feature in this class of materials. Notably, within the energetically favorable ferromagnetic structures, we find that two structures have very high stabilization energies for ferromagnetic order, one having the highest predicted so far for this class of materials. Finally, we find that several structures are half-metals, and that one in special is a half-zero-gap semicondutor.

Since the last decades magnetic properties have been observed in many materials in which there is no transition metal or rare earth element, that is, no d or f electrons [1]. For instance, numerous previous works have reported magnetic properties in two-dimensional carbon based materials such as graphene-based fragments, nanoribbons, and defective sheets [2], in carbon nanotubes [3], and, more recently, in graphitic carbon nitrides [4, 5]. From a fundamental viewpoint this d^0 magnetism has attracted great attention due to the interest in disclosing the physical mechanisms from which these properties emerge.

Moreover, carbon-based materials have also attracted enormous interest for applications in spintronic devices [6, 7]. For instance, the high electronic mobility and weak spin orbit coupling of graphene [8, 9] make it a promising spin channel material. In fact, graphene spin valve devices have been fabricated, exhibiting room temperature nanosecond spin lifetimes and diffusion lengths of micrometers [10, 11]. In addition, another class of two-dimensional materials known as transition-metal dichalcogenides [12] have shown useful properties for applications in spintronics. In particular, MoS_2 monolayers exhibit direct band gap and larger spin-orbit coupling than graphene, which in turn leads to larger spin orbit scattering lenghts [12, 13]. Despite of these spin channel candidates, carbon-based half-metals such as graphitic carbon nitrides [14, 15] have been proposed as an alternative to usual ferromagnet electrodes towards metal-free spintronics.

Graphitic carbon nitrides based on s-triazine or tri-s-triazine subunits, often denoted by g-C_3N_4, are two-dimensional layered nonmagnetic semiconductors with graphene-like structure containing uniform periodic nanopores. Despite its great potential as a photocatalyst [16, 17], previous theoretical works have also proposed alternatives to induce magnetic ordering in these materials. For instance, hydrogen chemisorption [18, 19], carbon doping [4, 14], periodic large pores [22, 23], and fractal morphology [15] may give rise to magnetic carbon nitride structures. From the experimental side, the synthesis of the theoretical predicted ferromagnetic g-C_4N_3 [4] and the experimental observation of room temperature ferromagnetism in g-C_3N_4 nanosheets have been recently reported [5]. In the present work, we investigate, by means of first principles calculations, the electronic and magnetic properties of distinct graphene-like carbon nitride structures. Our results indicate that, among the considered set of twenty eight structures obtained through a simulated annealing procedure, there are twenty one structures with energetically favorable magnetic phases, where nine of them are ferromagnetic. The band structure calculations also suggest that the nonmagnetic states of several structures present Stoner-like instabilities, while the ferromagnetic phases of several other have half-metallic properties.

Our proposed carbon nitride structures have the morphology of a honeycomb lattice, where each lattice site can be a carbon atom, a nitrogen atom, or a vacant site. These structures are denoted by the general formula $C_xN_yv_z$, where x,y, and z define the number of carbons, nitrogens, and vacancies, respectively, in unit cells of eighteen sites. We considered twenty eight distinct (x, y, z) stoichiometries, and for each stoichiometry we first obtained a minimum-energy structure through a Monte Carlo simulated annealing procedure [29]. In this annealing procedure, we obtained approximately 10^5 configurations for each distinct (x, y, z) stoichiometry, from which we selected the ones with lowest energy applying the Metropolis criterion. This criterion changes during the annealing since the temperature is reduced as a function of the number of Monte Carlo steps. Throughout the Monte Carlo calculations the total energy of each structure was calculated from an empirical bond-couting model, parametrized from ab initio calculations, which takes into account the distinct bond energies presented in each structure and the additional energy induced by nitrogen doping.

Further, we performed first principles calculations to investigate the electronic and magnetic properties of each low-energy structure. Our first principles calculations were perfomed within the spin-polarized density func-

Physical Chemistry Chemical Physics Accepted Manuscript

tional theory (DFT) [24], employing the generalized-gradient approximation (GGA) [27], as implemented in SIESTA code [26]. To describe electron-ion interaction we used norm-conserving pseudopotentials [25]. The equilibrium geometries of each structure were further relaxed by using the conjugated gradient scheme within a force convergence criterion of 0.02 eV/Å, where the total energy was converged by using a set of 8 special k-points to the Brillouin zone sampling [28]. In addition, we investigated the stability of the ferromagnetic structures by means of first-principles Molecular dynamics, annealing the structures from 300 K to 273 K. For the distorted structures, further optimization using conjugated gradient scheme were done. Finally, the electronic and magnetic properties were investigated using a set of 36 special k-points and $2x2$ supercells to avoid spurious effects on the magnetic properties.

For each structure we addressed the energetic stability of the nonmagnetic, antiferromagnetic (AFM) and ferromagnetic (FM) phases. The magnetic ordered configurations were simulated starting with a spin-polarized calculation considering a predefined spin density. For those structures with stable magnetic state, we calculate the energetic stabilization driven by the formation of a magnetic ordered state, which is given by

$$\epsilon_s = E_m - E_{nm}, \quad (1)$$

where E_m and E_{nm} correspond to the total energy of the magnetic and nonmagnetic phases, respectively. The structures with energetically favorable magnetic phases ($\epsilon_s < 0$) are represented by triangles in the ternary diagram shown in Fig. 1. In the same diagram we represent the nonmagnetic structures by circles ($\epsilon_s > 0$). Moreover, these energies suggest a set of twenty two energetically favorable magnetic carbon nitride structures.

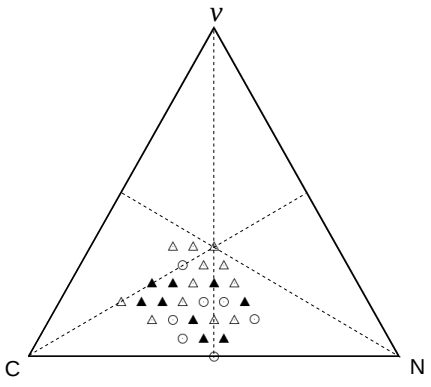

FIG. 1. Magnetic phase ternary diagram of graphene-like carbon nitride ($C_xN_yv_z$) structures. Antiferromagnetic and ferromagnetic phases are represented by empty and full triangles, respectively. Nonmagnetic structures are represented by empty circles.

To investigate the energetic stability of these magnetic phases, we further calculate the energy difference between the FM and AFM configurations, for each structure, as given by

$$\epsilon_o = E_{afm} - E_{fm}, \quad (2)$$

where E_{afm} and E_{fm} are the total energies of the same structure, considering AFM and FM configurations, respectively. Interestingly, based upon the calculated values of ϵ_o, we find a set of twelve structures with an energetically favorable AFM phase ($\epsilon_o < 0$): $C_7N_9v_2$, $C_8N_8v_2$, $C_{11}N_5v_2$, $C_{12}N_3v_3$, $C_9N_6v_3$, $C_6N_8v_4$, $C_8N_6v_4$, $C_6N_7v_5$, $C_7N_6v_5$, $C_6N_6v_6$, $C_7N_5v_6$, and $C_8N_4v_6$. These structures are represented by empty triangles in the ternary diagram shown in Fig. 1. In addition, we find a set of nine structures with an energetically favorable FM phase ($\epsilon_o > 0$): $C_8N_9v_1$, $C_9N_8v_1$, $C_9N_7v_2$, $C_6N_9v_3$, $C_{10}N_5v_3$, $C_{11}N_4v_3$, $C_7N_7v_4$, $C_9N_5v_4$, and $C_{10}N_4v_4$, which are represented as full triangles in the same diagram. It is important to mention that the $C_7N_7v_4$ structure obtained through or simulated annealing procedure corresponds to the same structure previously investigated in refs. [20, 30]. Table I presents the calculated ϵ_s and ϵ_o values for the FM structures, including the g-C_4N_3 (carbon doped g-C_3N_4) proposed by Du *et al.* [14].

TABLE I. Magnetic moment per supercell (m), and calculated energies (ϵ_s and ϵ_0), in meV, for structures which have energetically favorable ferromagnetic phase ($\epsilon_o > 0$). m is given in μ_B units.

x y z	y/x	m	ϵ_s	ϵ_0
8 9 1	1.13	2.35	-165.9	65.9
9 8 1	0.89	2.61	-121.2	4.2
9 7 2	0.78	4.00	-320.3	145.6
6 9 3	1.50	12.00	-1370.1	600.2
10 5 3	0.50	4.00	-233.2	61.1
11 4 3	0.36	4.00	-1069.3	136.7
7 7 4	1.00	4.00	-376.4	84.8
9 5 4	0.56	8.00	-494.5	–
10 4 4	0.40	9.98	-1467.3	248.9
g-C_4N_3	0.75	4.00	-413.1	326.9

From table I we observe that the g-C_4N_3 is found to be ferromagnetic with 1 μ_B per formula unit, in good agreement with the results of Du *et al.* [14]. For the $C_7N_7v_4$, we find 1 μ_B per formula unit, and that the ferromagnetic state is 84.8 meV more stable than the antiferromagnetic, in good agreement with previous results [20].

Fig. 2 shows a plot of the magnetic moment per atom ($m/(x+y)$) of the ferromagnetic structures as a function of the N/C ratio (y/x). Two features can be observed in this figure. First, most of the $m/(x+y)$ values are in the vicinity of 0.05 μ_B/atom, suggestive of a common order of magnitude for the magnetization of C-N layers. Second, if we disregard the structure $C_6N_9v_3$, the $m/(x+y)$ values show an overall trend of decreasing magnetic moments per atom upon increasing the relative concentra-

Physical Chemistry Chemical Physics Accepted Manuscript

tion of nitrogen, as can be seen in Fig. 2. We mention that a similar trend was recently observed experimentally in nitrogen-doped graphene domains [21].

Among our newly found ferromagnetic structures, $C_6N_9v_3$ and $C_{10}N_4v_4$ structures present larger energetic stabilization, as seen in table I, due to the formation of magnetic ordered states. In especial, we find that the ferromagnetic state of the former is 273 meV more stable than the ferromagnetic configuration of g-C_4N_3, and that this structure presents a magnetic moment of 3 μ_B per formula unit. The ferromagnetic state of $C_{10}N_4v_4$ structure is found to be 78 meV less stable than the ferromagnetic state of g-C_4N_3, while the remaining structures present less stable ferromagnetic states. These findings indicate the possibility of a carbon nitride structure with a more stable ferromagnetic phase than the ferromagnetic phase of g-C_4N_3.

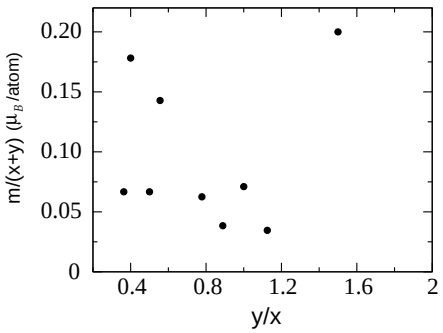

FIG. 2. Magnetic moments per atom $(m/(x+y))$ as a function of relative concentration of nitrogen (y/x) of the graphene-like carbon nitride ($C_xN_yv_z$) structures which have energetically favorable FM phase ($\epsilon_o > 0$).

The calculated equilibrium geometries and spin densities, of the ferromagnetic structures (excluding the $C_9N_8v_1$ structure), are shown in Fig. 3. It is important to mention that the $C_9N_8v_1$ structure will not be considered in our following investigation due to its very small value of $\epsilon_o = 4.2$ meV. From the spin density shown in Fig. 3(a) we observe the magnetic moments of g-C_4N_3 come mainly from the in-plane p_x and p_y orbitals of pyridinic nitrogens, also in good agreement with the findings of ref. [14].

Similar to g-C_4N_3, the magnetic moments of $C_9N_7v_2$, $C_6N_9v_3$, $C_{10}N_5v_3$, and $C_7N_7v_4$ originate mainly from the p_x and p_y orbitals, as can be seen in Fig. 3(c), (d), (e) and (g), respectively. In contrast, as shown in Fig. 3(b), in the structure $C_8N_9v_1$ the magnetic moments originate mainly from p_z orbitals associated with graphitic carbon and nitrogen atoms in the "bulk" part of the structure. In Fig. 3 (f), (h), and (i) we notice a different feature. Indeed, the carbon dangling bonds in $C_{11}N_4v_3$, $C_9N_5v_4$, and $C_{10}N_4v_4$ structures give rise to local magnetic moments due to the unpaired electron.

In order to investigate the physical mechanism responsible for the instability of the nonmagnetic phases, we performed band structure calculations for the nonmagnetic states of those ferromagnetic structures. We find that the nonmagnetic state of $C_8N_9v_1$, $C_7N_7v_4$, and $C_9N_5v_4$ structures present peaked density of states at around the Fermi level, as can be seen in Fig. 4. The high density of states at around E_F reveals a Stoner-like instability of the nonmagnetic phase of these structures. In particular, in $C_8N_9v_1$ we observe that this instability is related with states which are mostly due to graphitic carbon atoms. Meanwhile, in $C_7N_7v_4$ these states are mostly due to pyridinic nitrogens. For $C_9N_5v_4$ structure, we observe that the defective carbon atoms contribute more to these states than the pyridinic nitrogens. Similarly, such high density of states was found for the additional structures, although the density of states is not peaked at around the Fermi level in these cases. Overall, these findings are in accordance with the spin density feature presented in Fig. 3.

Finally, we investigate the effects of the magnetic ordering on the electronic properties of those structures. Here, we performed band structure calculations for the ferromagnetic states. A main feature in our band structures for $C_8N_9v_1$ (shown in Fig. 5), $C_{11}N_4v_3$, $C_9N_5v_4$, and $C_{10}N_4v_4$ structures, are the electronic levels with spin broken symmetry. For the $C_8N_9v_1$ structure we obtained semi-ocuppied levels, which accounts for the metallic nature of this system, while for the other structures we find band gaps of 0.25, 0.05, and 0.09 eV, respectively. On the other hand, as shown in Fig. 6, the calculated band structures of $C_9N_7v_2$, $C_6N_9v_3$, and $C_{10}N_5v_3$ present a different feature.

Interestingly, these band structures reveal that for the spin-up component (solid lines) there are band gaps of 0.24, 0.78, and 1.14 eV for $C_9N_7v_2$, $C_6N_9v_3$, and $C_{10}N_5v_3$ respectively. Further, for the $C_9N_7v_2$ and $C_6N_9v_3$ structures, one should notice there is no band gap for the spin-down component (dashed lines) and a considerable density of states at the Fermi level, such as in a half-metal. Such a similar feature was also found by Du *et al.* [14] for the g-C_4N_3. Surprisingly, we find that the spin-down component of the ferromagnetic state of $C_{10}N_5v_3$ presents an unusual feature. In fact, for this spin component we observe a graphene-like dispersion relation at around the Fermi level, as shown in the diagram in Fig. 6(d). In particular, we find two Dirac-like points along the $\Gamma - M$ and $\Gamma - K$ directions in the Brillouin zone, as can be seen in Fig. 6(c). Thus, our results indicate that this system can be considered as a half-zero-gap semiconductor.

In summary, we have investigated by means of first principles calculations the magnetic and electronic properties of graphene-like carbon nitride structures. Among our set of structures, our results suggest there are twelve structures with energetically favorable antiferromagnetic phase and nine with ferromagnetic phase. Notably,

Physical Chemistry Chemical Physics Accepted Manuscript

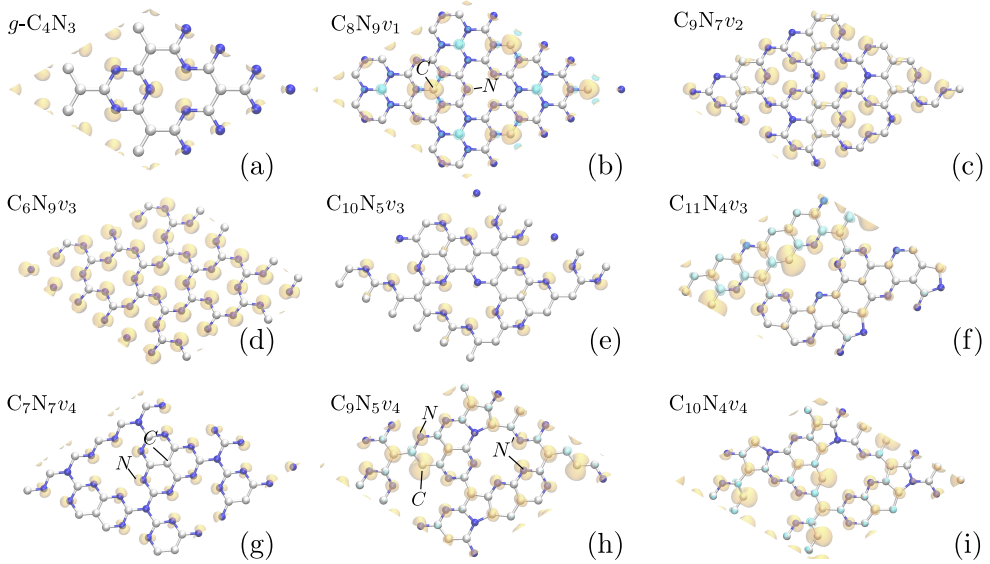

FIG. 3. (Color online) Equilibrium geometries (shown in $2x2$ unit cells) and spin densities ($\Delta\rho = \rho_{up} - \rho_{down}$) of (a) g-$C_4N_3$, (b) $C_8N_9v_1$, (c) $C_9N_7v_2$, (d) $C_6N_9v_3$, (e) $C_{10}N_5v_3$, (f) $C_{11}N_4v_3$, (g) $C_7N_7v_4$, (h) $C_9N_5v_4$, and (i) $C_{10}N_4v_4$. Carbon and nitrogen atoms are represented by white and blue spheres. Isosurfaces, in yellow ($\Delta\rho > 0$) and cyan ($\Delta\rho < 0$), correspond to spin densities of (a) 0.02, (b)0.002, (c)(f) 0.004, (d)(e)(g) 0.01, and (h)(i) 0.009 $e/bohr^3$.

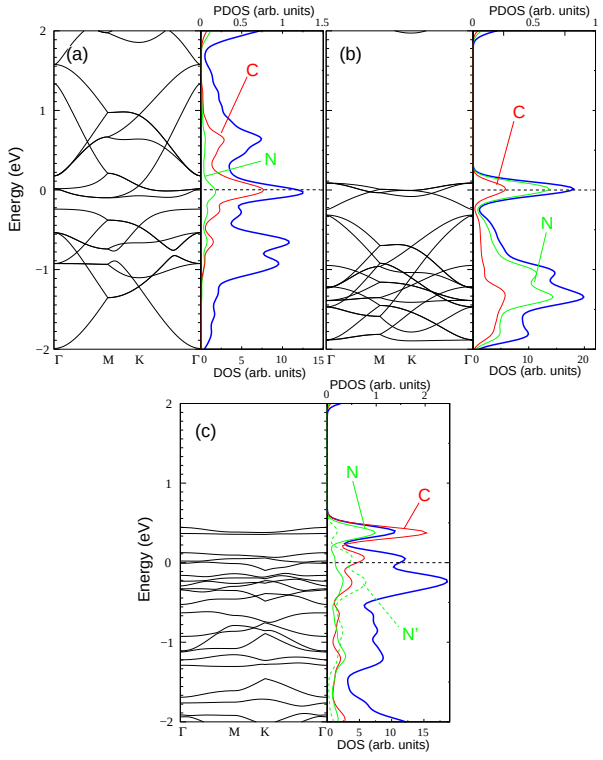

FIG. 4. (Color online) Calculated band structures, total (blue lines) and projected density of states of the nonmagnetic phase of (a) $C_8N_9v_1$, (b) $C_7N_7v_4$, and (c) $C_9N_5v_4$ structures. In the latter the states were projected on carbon (red lines) and nitrogen atoms (green lines) marked in Fig. 3.

within the energetically favorable ferromagnetic structures, we find that $C_{10}N_4v_4$, and $C_6N_9v_3$ may have high Currie temperatures as the previous magnetic carbon nitride structures. Our band structure calculations, for the nonmagnetic phase of several structures, indicates that these states present Stoner-like instabilities. Finally, we obtained the majority of these ferromagnetic structures remain metallic, where in special several ones may give rise to free-metal magnetic half-metals or even a half-zero-gap semiconductor.

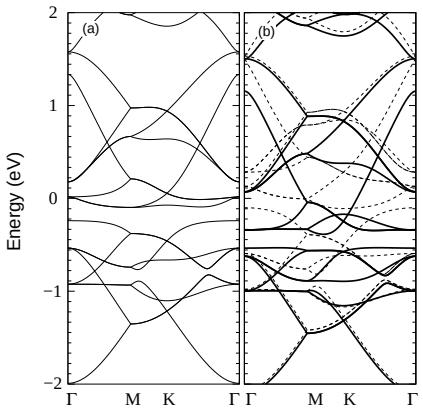

FIG. 5. Calculated band structures of the (a) nonmagnetic and (b) ferromagnetic phases of $C_8N_9v_1$. In the latter solid (dashed) lines represent the spin-up (spin-down) components.

We acknowledge support from the Brazilian agencies CNPq, FAPEMIG, CAPES, and from the project INCT de Nanomateriais de Carbono.

Physical Chemistry Chemical Physics Accepted Manuscript

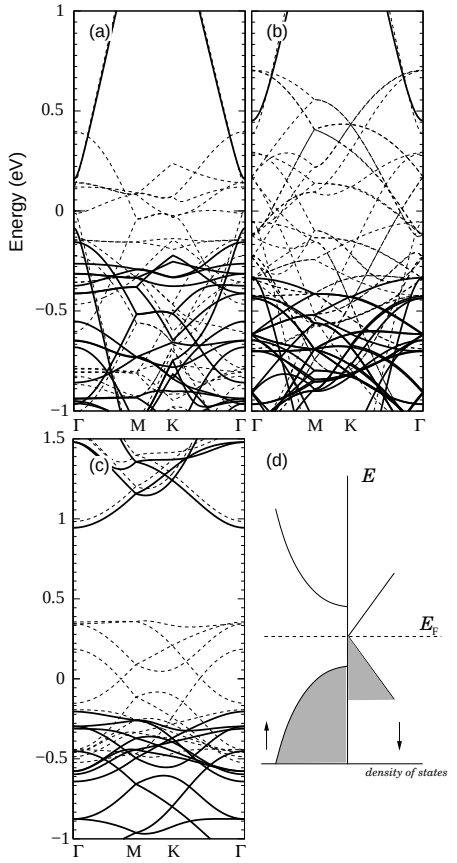

FIG. 6. Calculated band structures of the ferromagnetic phases of (a) $C_9N_7v_2$, (b) $C_6N_9v_3$, and (c) $C_{10}N_5v_3$. Solid (dashed) lines represent the spin-up (spin-down) components. (d) Energy band diagrams for a half-zero-gap semiconductor.

* walber@fisica.ufmg.br

[1] T. L. Makarova and F. Palacio, *Carbon based Magnetism: An Overview of the Magnetism of Metal Free Carbon-based Compounds and Materials*, Elsevier, Amsterdam (2006).
[2] O. V. Yazyev, Rep. Prog. Phys. **73**, 056501 (2010).
[3] S. S. Alexandre, M. S. C. Mazzoni, and H. Chacham, Phys. Rev. Lett. **100**, 146801 (2008).
[4] B. J. S. Lee, X. Wang, H. Luo, and S. Dai, Adv. Mater. **22**, 1004 (2010).
[5] D. Gao, Q. Xu, J. Zhang, Z. Yang, M. Si, Z. Yan, and D. Xue, Nanoscale **6**, 2577 (2014).
[6] D. Pesin and A. H. MacDonald, Nat. Mater. **11**, 409 (2012).
[7] W. Han, R. K. Kawakami, M. Gmitra, and J. Fabian Nat. Nanotechnology **9**, 794 (2014).
[8] K. S. Novosolev, A. K. Geim, S. V. Morozov, D. Jiang, Y. Zhang, S. V. Dubonos, I. V. Grigorieva, and A. A. Firsov, Science **306**, 666 (2004).
[9] A. H. Castro-Neto, F. Guinea, N. M. R. Peres, K. S. Novosolev, and A. K. Geim, Rev. Mod. Phys. **81**, 109 (2009).
[10] M. Drögeler, F. Volmer, M. Wolter, B. Terrés, K. Watanabe, T. Taniguchi, G. Güntherodt, C. Stampfer, and B. Beschoten, Nano Lett. **14**, 6050 (2014).
[11] S. Roche, J. Åkerman, B. Beschoten, J.-C. Charlier, M. Chshiev, S. P. Dash, B. Dlubak, J. Fabian, A. Fert, M. Guimarães, F. Guinea, I. Grigorieva, C. Schönenberger, P. Seneor, C. Stampfer, S. O. Valenzuela, X. Waintal, and B. van Wess, 2D Materials **2**, 030202 (2015).
[12] S. Z. Butler, S. M. Hollen, L. Cao, Y. Cui, J. A. Gupta, H. R. Guitérrez, T. F. Heinz, S. S. Hong, J. Huang, A. F. Ismach, E. J.-Halperin, M. Kuno, V. V. Plashnitsa, R. D. Robinson, R. S. Ruoff, S. Salahuddin, J. Shan, M. G. Spencer, M. Terrones, W. Windl, and J. E. Goldberger, ACS Nano **7**, 2898 (2013).
[13] N. Zibouche, A. Kuc, J. Musfeldt, and T. Heine, Ann. Phys. **526**, 395 (2014).
[14] A. Du, S. Sanvito, and S. C. Smith, Phys. Rev. Lett. **108**, 197207 (2012).
[15] A. Wang and M. Zhao, Phys. Chem. Chem. Phys. **17**, 21837 (2015).
[16] X. Wang, K. Maeda, A. Thomas, K. Takanabe, G. Xin, J. M. Carlsson, K. Domen, and M. Antonietti, Nat. Mater. **8**, 76 (2009).
[17] J. Liu, Y. Liu, N. Liu, Y. Han, X. Zhang, H. Huang, Y. Lifshitz, S.-T. Lee, J. Zhong, Z. Kang, Science **347**, 970 (2015).
[18] H. Qiu, Z. Wang, and X. Sheng, Phys. Lett. A **377**, 347 (2013).
[19] H. Qiu, Z. Wang, X. Sheng, Physica B **421**, 46 (2013).
[20] X. Zhang, M. Zhao, A. Wang, X. Wang and A. Du, J. Mater. Chem. C **1**, 6265 (2013).
[21] Y. Ito, C. Christodoulou, M. V. Nardi, N. Koch, M. Kläui, H. Sachdev, and K. Müllen, J. Am. Chem. Soc. **137**, 7678 (2015).
[22] X. Li, J. Zhou, Q. Wang, Y. Kawazoe, and P. Jena, J. Phys. Chem. Lett. **4**, 259 (2013).
[23] X. Zhang, A. Wang, and M. Zhao, Carbon **84**, 1 (2015).
[24] W. Kohn and L. J. Sham, Phys. Rev. **140**, A1133 (1965).
[25] N. Troullier and J. L. Martins, Phys. Rev. B **43**, 1993 (1991).
[26] J. M. Soler, E. Artacho, J. D. Gale, A. Garcia, J. Junquera, P. Ordejón, and D. Sánchez-Portal, J. Phys. Condens. Matter **14**, 2745 (2002).
[27] J. P. Perdew, K. Burke and M. Ernzerhof, Phys. Rev. Lett. **77**, 3865 (1996).
[28] H. J. Monkhorst and J. P. Pack, Phys. Rev. B **13**, 5188 (1976).
[29] W. H. Brito, Joice da Silva-Araújo, and H. Chacham, J. Phys. Chem. C **119**, 19743 (2015).
[30] X. Li, S. Zhang, and Q. Wang, Phys. Chem. Chem. Phys. **15**, 7142 (2013).

Physical Chemistry Chemical Physics Accepted Manuscript